Organic Process Research & Development **2005**, *9*, 894–901

Control of the Particle Properties of a Drug Substance by Crystallization Engineering and the Effect on Drug Product Formulation

Soojin Kim,* Bruce Lotz, Mark Lindrud, Kevin Girard, Terence Moore, Karthi Nagarajan, Mario Alvarez, Tu Lee, Faranak Nikfar, Martha Davidovich, Sushil Srivastava, and San Kiang

Pharmaceutical Development, Bristol-Myers Squibb Company, New Brunswick, New Jersey 08903, U.S.A.

Abstract:

A study of the process−property−performance relationship of a Bristol-Myers Squibb drug substance led to successful development of crystallization and drying processes that produce crystals with desired and consistent physical properties. A controlled crystallization technique was developed to obtain well-defined, large crystals with a narrow particle size distribution. This crystallization process provided a less compressible filter cake for effective cake washing and deliquoring and afforded an easily dried product with desired powder properties. To preserve the quality of the crystals during drying, a drying protocol using low shear agitation was developed. This protocol prevented crystal attrition during drying, which was shown to adversely affect the formulation process and, thus, drug product performance. API crystals prepared by this method consistently resulted in excellent formulation processing and drug product performance.

Introduction

Crystallization is a critical unit operation in the manufacture of pharmaceutical compounds. It is often a key isolation step or a purification process in the synthesis of an active pharmaceutical ingredient (API). Crystallization of an API in particular is critical for product qualities such as chemical purity and correct polymorphic form, which need to be strictly controlled to meet set specifications.

Optimization of the crystallization process for an API is important not only for the key product requirements mentioned above but also for process efficiency. The API crystallization process and crystal properties have a significant effect on downstream processing. For example, excess fines or wide particle size distribution may cause slow filtration and inefficient drying, which may be a major bottleneck of the entire manufacturing process. It is often necessary to modify the crystallization process to control particle properties to facilitate downstream operations.[1,2]

Physical properties such as particle size, crystal habit, and surface properties are important aspects of API product quality and must be considered with great care and attention during the development of an API crystallization process. The effort of modifying a crystallization process to effect changes in the physical properties of crystals is often called particle engineering.[3,4] At Bristol-Myers Squibb (BMS), particle engineering has been carried out for many API to obtain the desired particle size or habit to meet biopharmaceutical performance requirements.[3,5] For example, for insoluble or dissolution-limited drug substances, small particle size is necessary to maximize surface area to enhance bioavailability.[6−8] For development of drug product processes, particle uniformity may be critical to the homogeneity of a blend or granulation, which directly correlates with the content uniformity and dissolution properties of the drug product. In addition, API crystal properties such as particle size distribution, habit, and surface properties have a large effect on bulk powder properties, which may affect formulation operations such as blending, granulation, and compaction.[9−11] Therefore, having consistent and optimal physical properties of the API is essential for development of formulation processes to produce consistent and reliable drug products.

Design of crystallization processes is aimed at achieving drug substances with desired characteristics in consistently high quality. On the other hand, preserving the crystal quality and key physical properties throughout the downstream processing steps, such as filtration, drying, and delumping, may be a challenging task. For example, undesirable form change, particle size reduction, or agglomeration may arise as a result of the downstream processing and cause poor product performance or formulation behavior. In some cases, monitoring key particle properties during the processing steps following crystallization may be necessary and would allow identification of key processing parameters and their controls.

This paper discusses crystallization development of a BMS drug substance whose physical properties had a strong effect on formulation and drug product performance. This is a case study of development efforts to establish a controlled crystallization process for the API. The goal was to produce optimal crystal properties to facilitate filtration, drying, and powder handling and to develop a drying protocol to maintain

* Author for correspondence. Mailing address: Bristol-Myers Squibb, 1 Squibb Dr., New Brunswick, NJ 08903, U.S.A. Phone: (732) 227-7025. Fax: (732) 227-3003. E-mail: soojin.kim@bms.com.

(1) Mullin, J. W. *Crystallization*, 3rd ed.; Butterworth-Heinemann: Boston, 1993; p 421.
(2) Rossiter, A. P.; Douglas, J. M. *Chem. Eng. Res. Des.* **1986**, *64*, 175.
(3) Kim, S.; Wei, C.; Kiang, S. *Org. Process Res. Dev.* **2003**, *7*, 997.
(4) Dennehy, R. D. R *Org. Process Res. Dev.* **2003**, *7*, 1002.
(5) Kim, S.; Wei, C.; Kiang, S. *6th International Workshop on the Crystal Growth of Organic Materials*; Glasgow, 2003
(6) Rasenack, N.; Muller, B. W. *Pharm. Res.* **2002**, *19*, 1894.
(7) Kawashima, Y. *Adv. Drug Delivery Rev.* **2001**, *47*, 1.
(8) Kreuter, J. *Pharm. Acta Helv.* **1983**, *58*, 196.
(9) Mackin, L.; Sartnurak, S.; Thomas, I.; Moore, S. *Int. J. Pharm.* **2002**, *231*, 213.
(10) Feeley, J. C.; York, P.; Sumby, B. S.; Dicks, H. *Int. J. Pharm.* **1998**, *172*, 89.
(11) Dries, K.; Vromans, H. *Int. J. Pharm.* **2002**, *247*, 167.

Published on Web 10/29/2005

10.1021/op050091q CCC: $30.25

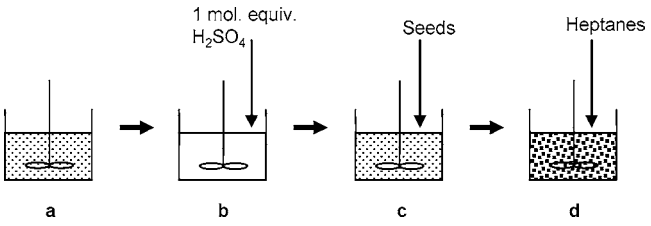

Figure 1. **Schematic illustration of the uncontrolled crystallization for the bisulfate salt formation. (a) Free base suspension in ethanol; (b) sulfuric acid addition followed by formation of homogeneous bisulfate salt solution; (c) seed addition followed by rapid crystallization; (d) heptanes addition for increased yield. A rapid, moderate exotherm, which includes both heat of reaction and heat of solution, is generated upon the addition of sulfuric acid with a temperature rise of about 3 °C in the lab. On scale, the exotherm is controlled through the incorporation of a slow acid addition.**

the integrity of the API crystals to achieve consistent formulation characteristics and performance of the drug product.

Crystallization Process Development

Uncontrolled Crystallization. The BMS compound, a bisulfate salt, is produced by a reactive crystallization involving salt formation between the free base and sulfuric acid. During early development, the crystallization process involved adding sulfuric acid to the free base suspended in ethanol. Addition of the acid caused the free base to dissolve and react to form the bisulfate salt in solution. Crystallization was then initiated by seeding, upon which precipitation of the bisulfate salt proceeded quickly due to high supersaturation of the bisulfate salt in ethanol. Heptanes were subsequently added as antisolvent to maximize the yield. The process is illustrated schematically in Figure 1.

Rapid crystallization under high supersaturation caused a large degree of uncontrolled nucleation and growth resulting in excessive fines and wide particle size distribution. A very slow filtration with inefficient washing was a major bottleneck of the overall process. In addition, the wet cake was highly compressible. When dried, the wet cake compacted into hard lumps and required extensive milling for further processing. An improved crystallization process was needed not only to enhance process efficiency and productivity but also for consistency in the physical properties of the API.

Controlled Crystallization. It is well-known that a rapid change of supersaturation, particularly in the initial stage of crystallization process, results in formation of a large number of nuclei and generally yields a nonuniform product.[12,13] While growth rates increase with a higher operating level of supersaturation, the increase in nucleation rate is more sensitive to the higher supersaturation level and plays the dominant role in the formation of particles, especially fines. Keeping the working level of supersaturation low to keep the nucleation rate low significantly improves the uniformity of product.

(12) Mullin, J. W.; Nyvlt, J. *Chem. Eng. Sci.* **1971**, *26*, 369.
(13) Mullin, J. W. *Crystallization*, 3rd ed.; Butterworth-Heinemann: Boston, 1993; p 389.

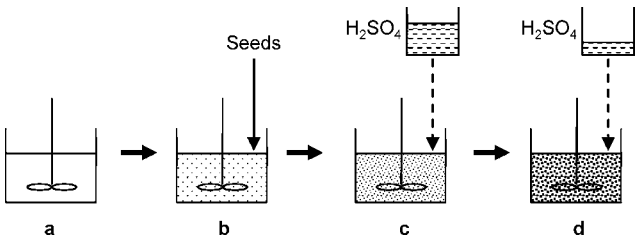

Figure 2. **Schematic illustration of the controlled crystallization with an incremental addition of sulfuric acid. (a) The free base solution in acetone/NMP; (b) the bisulfate seed crystal addition to the free base solution; (c) incremental addition of sulfuric acid; (d) the salt crystallization continues slowly with continuous addition of sulfuric acid.**

The elemental reactions for the reactive crystallization process for this compound may be written as

$$\text{FreeBase} + \text{Acid} \rightarrow \text{Salt(solution)}$$

$$\text{Salt(solution)} \rightarrow \text{Salt(crystal)}$$

For which the kinetics may be expressed simply

$$\text{Rate of reaction} = k_r C_{FB}^{a} C_{acid}^{b} \quad (1)$$

$$\text{Rate of crystallization} = k_g A(t) \Delta C_{salt(solution)}^{g} + k_n \Delta C_{salt(solution)}^{n} \quad (2)$$

where k_r, k_n, and k_g are the rate constants for the reaction, nucleation, and growth, respectively, $A(t)$ is the surface area for crystal growth, $C_{salt(solution)}$ and $\Delta C_{salt(solution)}$ are the concentration and supersaturation of the bisulfate salt dissolved in solution, and C_{FB} and C_{acid} are the free base and acid concentrations in solution.

It is obvious that the extent of the above reaction can be limited by limiting the amount of acid accessible for reaction. By controlling the addition rate of acid, one can obtain a measure of control over the rate of reaction and thus the rate of salt formation in solution which is equal to the rate of supersaturation change.

For controlled crystallization of the bisulfate salt, the free base was first dissolved in an acetone/*N*-methyl pyrrolidone (NMP) mixture which provided much better solubility for the free base than ethanol used in the early development process. Complete dissolution of the free base allowed adequate management of the supersaturation by controlling acid addition into the free base solution with seed crystals present. Figure 2 schematically shows the crystallization process utilizing incremental addition of acid to control the rate of reaction/crystallization. By carrying out the crystallization using this controlled acid addition method, rapid nucleation could be avoided, thereby reducing the amount of fines. Using this new crystallization process, the slow filtration problem was greatly alleviated.

Cubic Addition Crystallization. Further refinement of the controlled crystallization used "cubic addition" wherein the acid was added incrementally at a variable rate: slow at first and then gradually faster toward the end as the number of crystals and surface area available for growth increase. This crystallization protocol was designed to minimize the nucleation rate, thus encouraging particle growth onto seed crystals that serve as nuclei.

The cubic addition profile is analogous to the well-known cubic cooling profile in a temperature controlled crystallization, which is often used in general industrial applications as a simple approximation for controlled cooling crystallization.[13,14] Earlier reports[12,14] show the derivation of the following simplified equation:

$$T = T_{max} - (T_{max} - T_{min}) \times \left(\frac{t}{t_{total}}\right)^3 \quad (3)$$

where T is the temperature at time t, T_{max} and T_{min} are the starting and ending temperatures for the crystallization, and t_{total} is the total crystallization time.

In our case involving the BMS compound, the crystallization occurs as a result of a reaction controlled by the addition of sulfuric acid. The rate of crystallization, expressed as the rate of accumulation for the bisulfate salt crystals, $dC_{salt(cryst)}/dt$, is the sum of the crystal growth rate and the nucleation rate:

$$\frac{dC_{salt(cryst)}}{dt} = k_g A(t) \Delta C^g_{salt(solution)} + k_n \Delta C^n_{salt(solution)} \quad (4)$$

The rate of accumulation for the bisulfate salt dissolved in solution, $dC_{salt(solution)}/dt$, may be written as:

$$\frac{dC_{salt(solution)}}{dt} = k_r C^a_{FB} C^b_{acid} - k_g A(t) \Delta C^g_{salt(solution)} - k_n \Delta C^n_{salt(solution)} \quad (5)$$

Accumulation rate of the acid in solution may be expressed as

$$\frac{dC_{acid}}{dt} = F(t) - k_r C^a_{FB} C^b_{acid} \quad (6)$$

where $F(t)$ is the addition rate of acid. Equations 5 and 6 may be combined to give the following expression:

$$\frac{dC_{salt(solution)}}{dt} = -\frac{dC_{acid}}{dt} + F(t) - k_g A(t) \Delta C^g_{salt(solution)} - k_n \Delta C^n_{salt(solution)} \quad (7)$$

Assuming minimal nucleation and crystallization growth mainly onto added seed crystals, the nucleation term may be eliminated to give

$$\frac{dC_{salt(solution)}}{dt} = -\frac{dC_{acid}}{dt} + F(t) - k_g A(t) \Delta C^g_{salt(solution)} \quad (8)$$

The growth rate term may be replaced as a function of crystal size $L(t)$ and linear growth rate $G(t)$:

$$L(t) = L_{so} + G(t) \cdot t \quad (9)$$

where L_{so} is the seed size. Equation 8 then can be expressed as follows, analogous to the theoretical derivation reported previously:[14−16]

$$\frac{dC_{salt(solution)}}{dt} = -\frac{dC_{acid}}{dt} + F(t) - \frac{3W_{so}}{L_{so}^3} L^2(t) G(t) \quad (10)$$

where W_{so} is the mass of added seeds.

The accumulation term for the acid, dC_{acid}/dt, is expected to be negligible as the reaction itself is relatively fast compared to crystallization. In addition, as the crystallization rate is controlled by limiting acid addition, the accumulation term for bisulfate salt dissolved in solution, $dC_{salt(solution)}/dt$, should be negligible. Then the expression for the acid addition rate $F(t)$ can be simplified as

$$F(t) = \frac{3W_{so}}{L_{so}^3} (L_{so} + G \cdot t)^2 G \quad (11)$$

$F(t)$ is the molar flow rate of acid, which is proportional to the volume flow rate dV/dt. Equation 11 can then be rewritten as

$$\frac{dV}{dt} = \frac{3W_{so}}{L_{so}^3} V_m (L_{so} + G \cdot t)^2 G \quad (12)$$

where V_m is the molar volume of acid.

The linear growth rate G may be considered independent of t or L and dependent only upon supersaturation, as treated in the article by Jones and Mullin,[14] since the system is designed to maintain a low supersaturation and controlled growth throughout. Assuming the initial seed size L_{so} is small compared to the subsequent grown size, eq 12 can be integrated and reduced to the following expression:

$$V(t) = V_{total} \cdot \left(\frac{t}{t_{total}}\right)^3 \quad (13)$$

where V is the volume of sulfuric acid added during the elapsed time period t and V_{total} is total volume of acid charge. Equation 13 is an approximate equation for the optimal addition rate protocol for controlled crystallization, henceforth referred to as "the cubic addition protocol."

By controlling the acid addition rate according to the above expression, nucleation could be controlled within acceptable limits as the system maintained a constant low level of supersaturation. The slow initial acid addition rate was shown to favor crystal growth onto seeds over nucleation. As the crystallization progressed, the surface area available for growth increased at an increasing rate, thereby allowing acid to be added at an increasing rate without inducing significant nucleation. The cubic addition crystallization provided a less compressible filter cake, which aided in effective cake deliquoring and washing. Filtration and drying of the crystals were also greatly improved, and the crystals dried into a powder with excellent flow and bulk handling properties.

Crystal particle size and morphology were shown to be dependent upon the overall addition rate of sulfuric acid. The slower the overall addition rate, i.e., the longer the overall crystallization time, t_{total}, the larger the mean crystal size. The cubic addition protocol carried out over 6−8 h provided relatively larger, more well-defined crystals, along

(14) Jones, A. G.; Mullin, J. W. *Chem. Eng. Sci.* **1974**, *29*, 105.
(15) Jones, A. G. *Chem. Eng. Sci.* **1974**, *29*, 1075.
(16) Tavare, N. S.; Garside, J.; Chivate, M. R. *Ind. Eng. Chem. Process Des. Dev.* **1980**, *19*, 653.

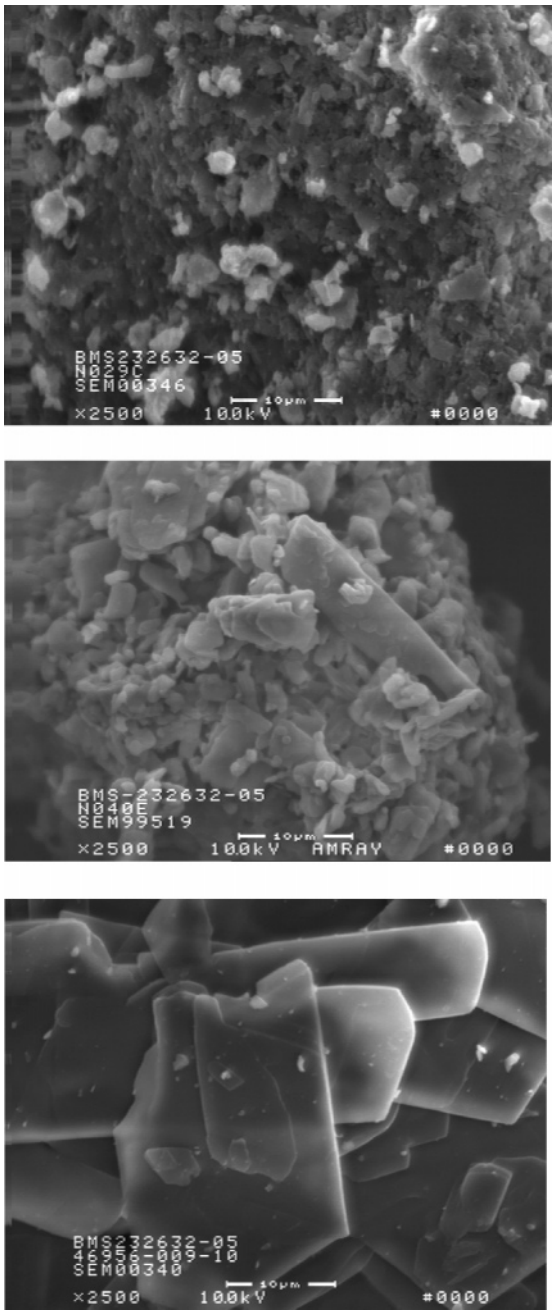

Figure 3. **Scanning electron micrographs of crystals from (a) uncontrolled crystallization; (b) linear addition crystallization; (c) cubic addition crystallization.**

with a narrower particle size distribution and fewer fines, than a constant addition rate crystallization. Figure 3 shows the scanning electron microscope (SEM) images of particles obtained from (a) uncontrolled crystallization showing highly aggregated fine particles compacted after filtration and drying, (b) linear addition crystallization showing somewhat increased particle size, and (c) cubic addition crystallization, which shows larger, well-defined crystals.

Seeding was demonstrated to be critical to the control of crystallization and also had an important effect on the final mean crystal size. A larger amount of seeds generally resulted in a greater mean particle size. This was probably because the large amount of seeds more effectively suppressed nucleation and promoted a growth-dominated environment,

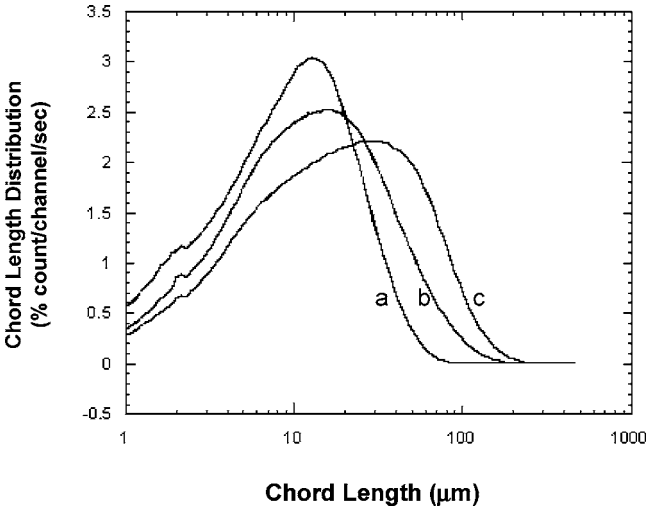

Figure 4. **Particle size distribution of crystals from (a) the linear addition protocol with 0.5 wt % seeding; (b) the cubic addition protocol with 0.5 wt % seeding; (c) the cubic addition protocol with 5 wt % seeding, as represented by chord length distribution. A chord length is a straight line between any two points on the edge of the particle, measured by a focused laser beam projected through a probe at a fixed velocity and rapidly scanned across particles.[17]**

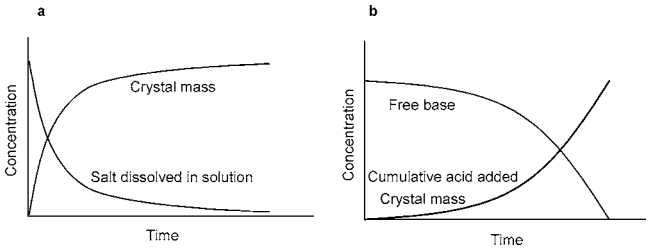

Figure 5. **Schematic representation of the changing concentrations of the dissolved species in solution and of the crystal mass for (a) the uncontrolled crystallization wherein all the acid is added at time zero and (b) the cubic addition crystallization wherein the acid addition follows a cubic (or third order of time) profile.**

whereas with a small amount of seeds, nucleation competed with crystal growth onto existing seeds. Figure 4 shows plots of the particle size distribution obtained from different experiments, as measured by Lasentec Focused Beam Reflectance Measurement (FBRM) of chord length which is a direct function of crystal dimensions. Chord length distribution is a representation of particle size distribution.[17,18] Figure 4 compares particle size distribution profiles from linear and cubic addition crystallizations carried out with different amounts of seeds.

To visualize the rate process of the cubic addition crystallization and to compare it to that of the uncontrolled crystallization described earlier, we can schematically illustrate the changing rates of free base or the dissolved bisulfate salt concentration in solution and salt crystal mass concentration during crystallization. Figure 5a portrays the uncontrolled crystallization wherein all the acid is added at once and the resulting bisulfate salt solution is highly

(17) Understanding and Utilizing FBRM: Focused Beam Reflectance Measurement, Lasentec, 1999, Mettler-Toledo.
(18) Ruf, A.; Worlitschek, J.; Mazzoti, M. *Part. Part. Syst. Charact.* **2000**, *17*, 167.

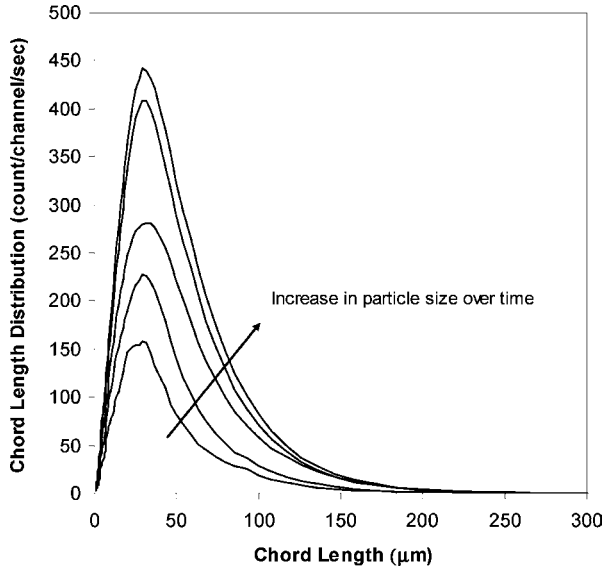

Figure 6. **Particle size distributions of crystals grown during the cubic addition crystallization of the bisulfate salt as represented by Lasentec FBRM chord length distribution.**

supersaturated at time zero. The crystallization process undergoes an exponential decrease of dissolved bisulfate salt concentration, which is inversely proportional to crystal mass concentration with a rapid initial increase, attributing to excessive nucleation and uncontrolled crystallization. On the other hand, the cubic addition case shown in Figure 5b experiences a slow initial decrease followed by a gradually faster decrease of the free base concentration, corresponding to a gradually increasing acid addition rate. The crystal mass also increases proportionally to the cumulative acid volume added, following a cubic (or third order of time) profile as shown in the figure. The particle size distribution of the crystals formed during the course of the cubic addition crystallization was monitored by Lasentec FBRM. Figure 6 displays the progressive increase in crystal dimensions over time indicating a growth-dominated crystallization process.

The controlled crystallization process using the cubic or incremental addition technique to limit the extent of reaction, and thus crystallization kinetics, may be applicable to any reactive crystallization involving reactions such as

(1) Acid + Base → salt crystals; or

(2) A + B → crystal product; or

(3) A + B + C → crystal product

where the reactants are liquids or dissolved in solvents, and the crystals precipitate as a result of the reaction. By controlling the extent of reaction using an incremental addition of one of the reactants into the solution of the other reactant, the supersaturation can be controlled within low limits to minimize nucleation.

The resulting crystals are generally larger and of better quality and have fewer fines and a narrower particle size distribution compared to those produced by uncontrolled crystallization techniques. The cubic addition crystallization technique has been successfully applied to several BMS compounds to produce crystals with optimal physical properties. The controlled cubic addition crystallization provided a less compressible filter cake, which aids in effective cake deliquoring and washing, as well as a more easily dried product with excellent powder properties than those obtained by uncontrolled or constant addition rate crystallization techniques. API crystals prepared by controlled crystallization also facilitated formulation due to improved bulk flowability, bulk density, and powder properties and handling.

Agitated Drying

Small scale lab experiments used tray drying of API crystals as a nonagitated flat cake layer. However, scale-up development and plant operations used agitated dryers that are more practical for large scale manufacturing where drying efficiency requires greater heat and mass transfer. During the course of development, the API was dried in different types of dryers to represent dryers in various manufacturing facilities. The agitated dryers evaluated for this API at BMS were a filter dryer, where the wet crystals are agitated with a pitched blade sweeping the cake bed close to the flat bottom surface; a conical dryer, where the material is agitated by a long, large center screw which revolves along the inner wall of a cone-shaped vessel while rotating on its own axis; and a tumble dryer, where the material is tumbled within a rotating double cone-shaped vessel. For all these dryers, drying was conducted at reduced pressure and with the vessel walls heated. Figure 7 shows pictures of the aforementioned dryers.

Parallel development of the API drying process and the formulation process revealed that the behavior of the finished API during formulation and the formulated product performance appeared to depend on the type of dryer and protocol used to dry the API. It was determined that the drug product formulated with API dried in a filter-dryer had a slower and more inconsistent dissolution performance, compared to that formulated with API dried in a tray dryer, a conical dryer, or a tumble dryer.

To maintain the integrity of crystal quality during the drying process, various crystal properties, which could affect the performance of the finished API, were monitored for changes as functions of agitation, extent of drying, and drying rate. The only notable change of physical properties during drying was the particle size. Particle size measurements at various stages of the API drying process indicated continuous particle size reduction when dried under agitation. The degree of attrition was greatest for crystals dried in the filter dryer, followed by the conical dryer and the tumble dryer, with minimal attrition by the tray dryer. Figure 8 shows the particle size distribution of crystals generated from the same cubic addition protocol, subsequently dried in the different types of dryers.

It is known that all agitated dryers introduce some degree of shear to crystals. The effect of agitation on crystal properties was tested in lab-scale dryers to define shear boundaries. The filter dryer with typical agitation caused the greatest degree of shear and crystal attrition that may adversely affect formulation behavior. Particle size monitoring during the drying experiments using slow or intermittent agitation indicated particle attrition can be reduced to

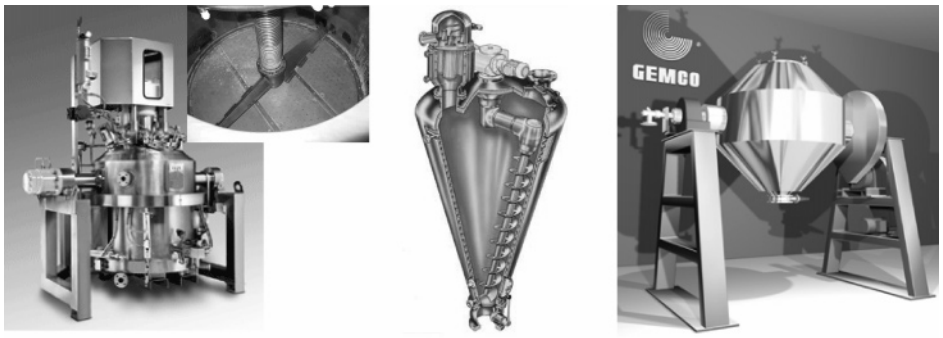

Figure 7. **Various agitated dryers for pharmaceuticals: (a) filter dryer (3V-Cogeim Inc.); (b) conical dryer (Bolz-Summix The MPE Group); (c) tumble dryer (Gemco Company Inc.).**

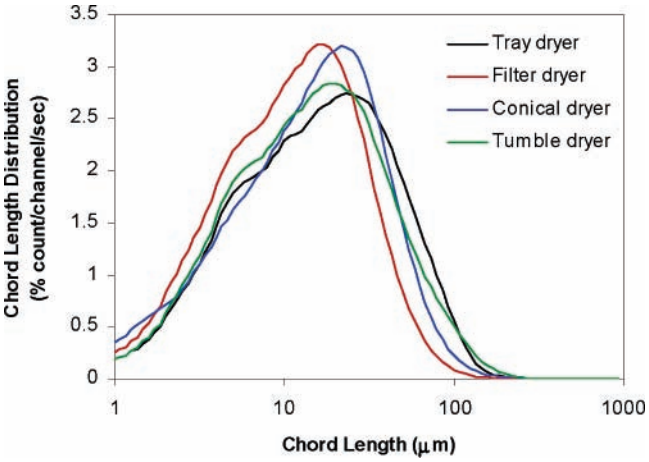

Figure 8. **Particle size distribution of crystals dried in different types of dryers.**

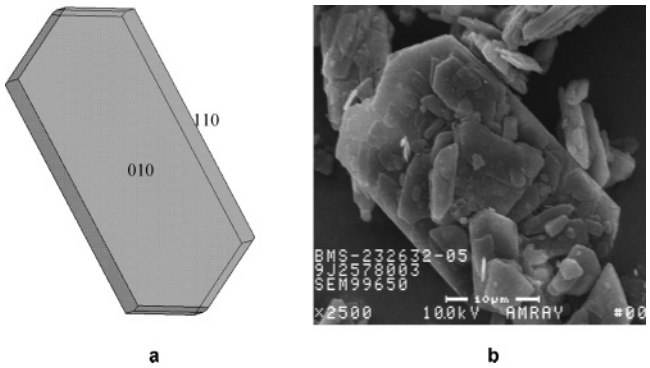

Figure 9. **Morphology of bisulfate salt crystals (a) from the molecular simulation by Cerius[2] and (b) from visual observation by SEM.**

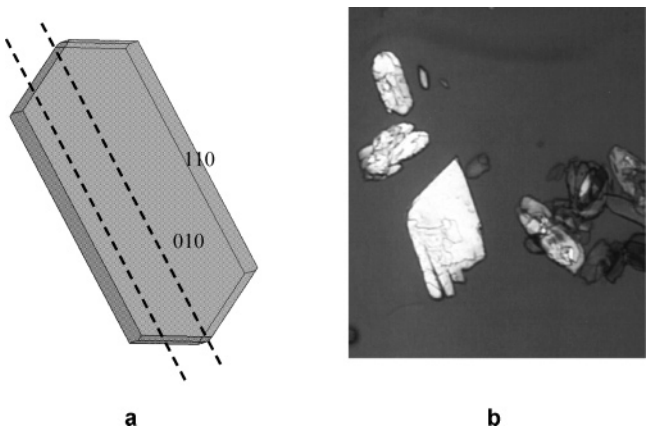

Figure 10. **(a) Morphology of bisulfate salt crystals from the molecular simulation with dashed lines indicating a likely direction of the crystal fracture; (b) optical microscope image of a crystal showing crack propagation in the same direction.**

acceptable levels by proper operation of a low shear drying protocol. The materials produced from the low shear agitation protocols in the filter dryer consistently presented acceptable dissolution performance, equivalent to material produced from the tray dryer.

Crystal Attrition

It was speculated that fracture of the plate-shaped primary particles exposed surfaces with functional groups affecting the granulation process in the formulation and therefore the quality of the granules produced. A detailed study of crystal properties revealed that broken crystals were more cohesive and easily agglomerated perhaps due to changed surface energetics. The cohesive nature of the crystals interfered with the granulation process and resulted in nonuniform API distribution in the granulation. This probably resulted in poor dissolution performance of capsules prepared from the granulation.

Molecular modeling was carried out on this compound for an in-depth study of crystal morphology and surface characteristics. The crystal structure and atomic coordinates obtained from single-crystal X-ray analysis were used for simulation of the crystal morphology by Cerius[2] software using the Attachment Energy method.[19,20] Figure 9 shows similarity of the simulated and actual morphology observed by SEM, both showing hexagonal thin plates.

Attachment energy, E_{att}, is defined as the energy released upon the attachment of a growth slice to a growing crystal surface. The growth rate of a crystal face is proportional to its attachment energy. Therefore, faces with the lowest attachment energies are the slowest growing and thus have the largest surface area and the most morphological importance. Attachment energy is calculated for a series of suitable slices (*hkl*) by performing a Donnay−Harker prediction.[21]

(19) Docherty, R.; Clydesdale, G.; Roberts, K. J.; Bennema, P. *J. Phys. D: Appl. Phys.* **1991**, *24*, 89.
(20) Berkovitch-Yellin, Z. *J. Am. Chem. Soc.* **1985**, *107*, 8239.
(21) Donnay, J. D. H.; Harker, D. *Am. Mineral.* **1937**, *22*, 463.

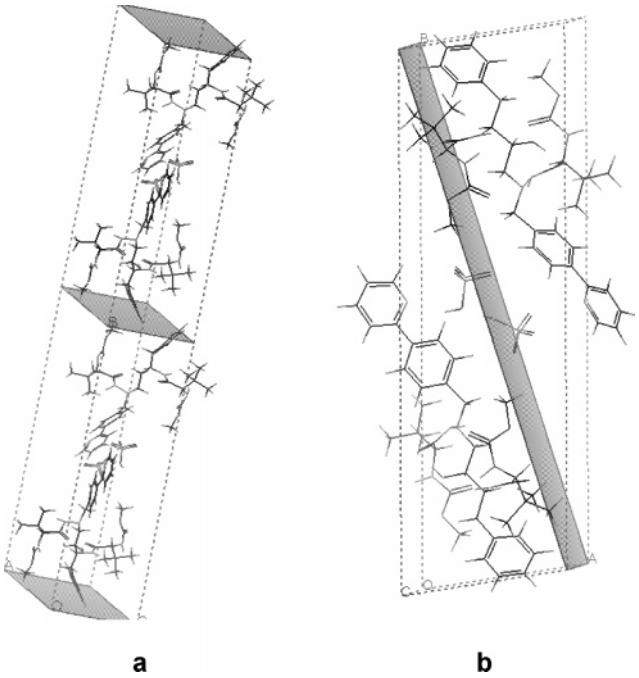

Figure 11. **Molecular arrangements of the bisulfate salt molecule with respect to (a) the (010) plane and (b) the (110) plane. Shaded areas represent the respective planes.**

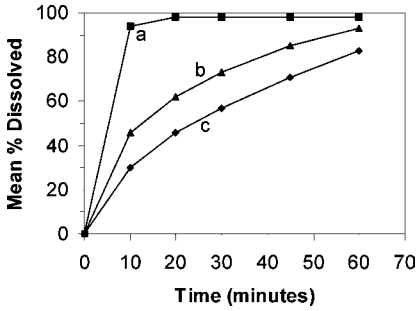

Figure 12. **Dissolution rates of capsules (the mean % dissolved of 6 capsules) manufactured using (a) a well performing API; (b) API from the filter dryer with normal agitation; (c) API subjected to the high shear milling.**

From the energy calculation and predicted growth rate, a center-to-face distance is assigned to each face, thereby predicting the final crystal habit.

Since the predicted and observed morphologies were similar, we could assign the (*hkl*) plane indices to the observed crystal faces and obtain detailed understanding of the molecular orientation with respect to different faces or slices of the crystal that could be visually observed. Under the optical microscope, the hexagonal thin plate-shaped crystals produced by the cubic addition crystallization appeared prone to breakage in the direction along the long axis of the hexagon, the (110) plane shown in Figure 9. Figure 10 illustrates the schematics of the fracture planes and the optical microscope image showing crack propagation.

The molecular orientation in the unit cell visualized by the Cerius[2] software, as shown in Figure 11, revealed the hexagonal face of the crystal with the largest surface area, the (010) plane, contains mostly hydrophobic functional

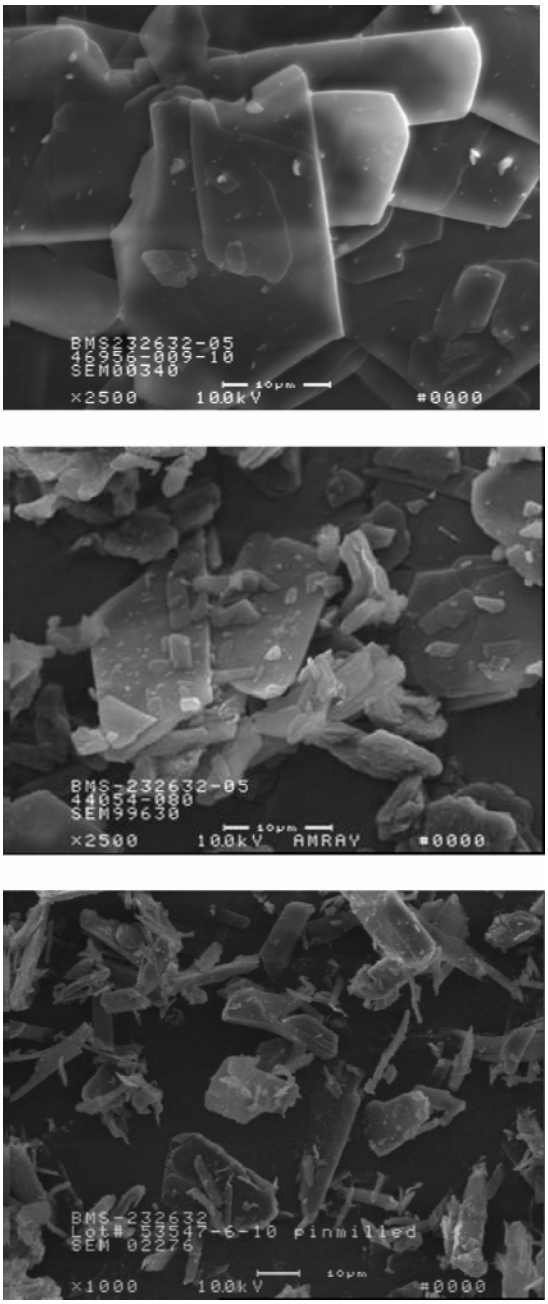

Figure 13. **SEM micrographs of the crystals from nonagitated drying (top), the crystals from the filter dryer with fast agitation (middle), and the crystals subjected to high shear milling (bottom).**

groups on the surface. On the other hand, the freshly exposed face upon crystal breakage, the (110) plane, contains largely the sulfate part of the molecule, which is considered hydrophilic. If excessive crystal breakage opens many fresh surfaces of the (110) plane, the increase in surface area containing hydrophilic groups is expected to alter the overall surface energetics of the bulk crystals. Such a change in surface energetics can affect surface−surface interactions among crystals as well as interaction of the crystals with water, which is used as the binder in the granulation process, and may be the root cause of the observed cohesive behavior/agglomeration.

An experiment was conducted to confirm the hypothesis that crystal attrition had a detrimental effect on the granulation process. A portion of an API batch that had been previously formulated to give an acceptable drug product dissolution profile was milled to deliberately cause attrition. The API was subjected to high shear milling, resulting in significant reduction of the mean particle size. The granulation using this API showed excessive agglomeration and cohesive behavior during preblending, indicating substantially changed surface properties. This batch had behavior similar to that of a batch subjected to considerable crystal attrition by agitated drying in the filter dryer. The formulated product using this milled batch also exhibited much slower dissolution. Figure 12 shows the dissolution profiles of the product manufactured using API lots from the filter dryer and from high shear milling, which are much slower than the dissolution rate of capsules from a typical API lot. Figure 13 shows the SEM micrographs of the crystals from nonagitated drying, the crystals from the filter dryer with fast agitation, and the crystals subjected to the high shear milling, showing similar morphology of the latter two which resulted in poor performance. The morphology of the broken crystals shown in the SEM is also consistent with that illustrated in Figure 10 showing a tendency of the crystals to break into strips or narrow pieces along the long axis.

This experiment clearly demonstrated that poor dissolution performance of drug product prepared from API dried in the filter dryer was caused by crystal attrition resulting from excessive shear due to agitation. This finding led to development of a drying protocol using conservative agitation to preserve crystal morphology and to minimize crystal attrition for all subsequent batches.

Conclusions

Crystallization, isolation, and drying processes of a BMS drug substance were developed to resolve the issues of wide particle size distribution, wet cake compressibility, slow filtration rate, wash efficiency, powder properties, and formulation problems. Crystals produced by the cubic addition crystallization protocol were more consistent in quality and size distribution and facilitated filtration, drying, and formulation. Drying experiments investigated the sensitivity of drug product performance to crystal breakage caused by agitation during drying. The study of crystal morphology and molecular orientation led to the understanding of changed surface energetics upon crystal fracture, which was shown to have an adverse effect on drug product performance. Agitated drying protocols were refined to reduce shear, thus minimizing the degree of attrition. API batches dried using the low shear protocols were shown to have excellent formulation characteristics and drug product dissolution performance.

Acknowledgment

We appreciate the collaboration with all the colleagues involved in this work at BMS.

Received for review June 3, 2005.

OP050091Q